

The formation mechanism of membranes prepared from the nonsolvent–solvent–crystalline polymer systems

Liao-Ping Cheng^a, Tai-Horng Young^{b,*}, Wen-Yuan Chuang^b, Li-Yen Chen^c, Leo-Wang Chen^c

^aDepartment of Chemical Engineering, Tamkang University, Taipei, Taiwan, ROC

^bInstitute of Biomedical Engineering, College of Medicine and College of Engineering, National Taiwan University, Taipei, Taiwan, ROC

^cDepartment of Chemical Engineering, National Taiwan University, Taipei, Taiwan, ROC

Received 1 October 1999; received in revised form 27 January 2000; accepted 15 May 2000

Abstract

Two different types of membranes were prepared by immersion–precipitation process in two nonsolvent–DMSO–poly(ethylene-*co*-vinyl alcohol) (EVAL) systems. The effect of nonsolvent on the resulting membrane structure was studied via scanning electron microscopy. On using 2-propanol as the nonsolvent, the membrane showed a homogeneous particulate morphology. If the nonsolvent was changed to water, the membrane structure was a typically asymmetric structure while the particulate morphology was suppressed. In order to understand the change of the obtained membrane structures, the phase diagrams of water–DMSO–EVAL and 2-propanol–DMSO–EVAL systems were contrasted at 25°C. Both crystallization-induced gelation and liquid–liquid demixing were observed and equilibrium crystallization lines are always positioned above the binodal boundaries. Moreover, the precipitation rate of the EVAL solution in 2-propanol and water were examined by the light transmission experiments and the local composition profiles of membrane solution during membrane formation were analyzed by using a ternary mass transfer model. Based on both thermodynamic behaviors and kinetic properties, the membrane structures obtained were discussed in terms of the sequence and mechanism of phase transformations during membrane formation. © 2000 Elsevier Science Ltd. All rights reserved.

Keywords: Crystalline polymer; Solid–liquid demixing; Liquid–liquid demixing

1. Introduction

Nowadays the immersion–precipitation technique is commonly used to prepare polymeric membranes. In this process, a homogeneous casting solution consisting of polymer and solvent is immersed into a nonsolvent coagulation bath. The exchange of solvent and nonsolvent due to diffusion causes the polymer solution to precipitate, by which the membrane is formed. It has been recognized that the thermodynamics and kinetics of liquid–liquid demixing in a nonsolvent–solvent–amorphous polymer system play important roles in determining the structure of asymmetric membranes [1–6]. However, besides liquid–liquid demixing, precipitation can take place by the process of solid–liquid demixing for crystallizable polymers to yield membranes exhibiting characters from both liquid–liquid demixing or/and solid–liquid demixing [7–10]. Liquid–liquid demixing results in the typical cellular morphology

with pores from polymer-poor phase surrounded by the membrane matrix from polymer-rich phase. Solid–liquid demixing is from crystallizable segments of the polymer to form membranes by linking of particles [11–14]. In general, crystallization is a slow process in comparison to liquid–liquid demixing [15] because of the time needed for orientation of the polymer molecule, both for nucleus formation and for growth. Consequently, the crystallization-controlled membrane structure has always been neglected. Although some reports described the formation mechanism of membrane morphology in terms of crystallization during the precipitation process [7–9,12–14,16], the complex phenomena including both thermodynamic and kinetic factors during the membrane formation almost restrict the studies to the experimental clarification of the relation between the membrane preparation conditions and the membrane structures. Therefore, the membrane formation mechanism of the crystalline polymer has not yet been elucidated in detail.

Commercially available poly(ethylene-*co*-vinyl alcohol) (EVAL) membranes have proved useful in hemodialysis [17,18], and particulate EVAL membranes are being

* Corresponding author. Tel.: +886-2-2397-0800, ext. 1455; fax: +886-2-2394-0049.

E-mail address: thyoung@ha.mc.ntu.edu.tw (T.-H. Young).

investigated for possible use in plasma protein separation and microfiltration [19,20]. As mentioned above, EVAL is a crystalline polymer [21,22], thus, it is rather difficult to determine the membrane structure only by the liquid–liquid demixing. To clearly understand the formation mechanism of EVAL membranes, knowledge of the equilibrium behavior in nonsolvent–solvent–EVAL systems is required. The most straightforward method of investigating thermodynamics, which is related to different types of phase separation during membrane formation, is to determine the phase diagrams of these solutions to elucidate the various membrane formation mechanisms. In the present work, the phase diagrams in the system of 2-propanol–DMSO–EVAL was measured at 25°C and compared to the system of water–DMSO–EVAL in our previous report [9]. These two systems were chosen because their phase diagrams were similar. Solid–liquid demixing is the favorable phase separation for the two systems on basis of the thermodynamic point of view. However, their membrane structures were totally different. This indicates that the unexpected behavior cannot be explained only by the phase diagram. Obviously, besides the thermodynamic behavior, it may be caused by diffusion kinetics of the system. Several authors have published theories that take into account the diffusion model to describe mass transfer during immersion precipitation [3–6,8,16]. In this work, the precipitation rate of the EVAL solution in 2-propanol and water were examined by the light transmission experiments and the diffusion trajectories in the phase diagram were analyzed by using a ternary mass transfer model. Based on both thermodynamic properties and kinetic properties for ternary system containing a crystalline polymer, the effect of nonsolvent on the membrane structures was discussed.

2. Experimental

2.1. Materials

Membranes were prepared by using EVAL polymer (105A, Kuraray Co. Ltd., Japan) having an average ethylene content of 44 mol%. Reagent-grade DMSO (Nacalai Tesque, Kyoto, Japan) was used as the solvent for EVAL and used as received. LC-grade 2-propanol (Alps Chem, Taiwan) and water (deionized and double distilled before use) were used as the nonsolvent.

2.2. Measurement of phase diagrams

The crystallization-induced gelation and liquid–liquid demixing boundaries were determined by cloud point method described in a previous publication [9]. Briefly, a specific amount of EVAL polymer (dried in an oven at 50°C) was mixed with a suitable amount of solvent–nonsolvent mixture and sealed in a Teflon-lined bottle (20 ml). This mixture was mechanically agitated at 60°C until a

clear homogeneous solution was obtained. The solution was then placed in an isothermal thermostat which was maintained at 25°C for a period of two weeks. With different nonsolvent contents, two types of phase separation may be observed: (i) the solution precipitates into a translucent or a white gel; (ii) solution becomes a clear liquid phase coexists with a white solid. For case (i), the equilibrium gelation point was identified as the composition at which a sharp increase in turbidity was observed by a turbidity bridge (Digital turbidimeter, Orbeco-Hellige, USA). The cloudy samples at these compositions are as a consequence of crystallization of EVAL molecules that have been proved by DSC scan in a previous publication [9]. For case (ii), gelation occurs in the polymer-rich phase after the liquid–liquid demixing. Therefore, the location of the liquid–liquid miscibility gap and gelation region will overlap in the phase diagram. The location of binodal in the ternary phase diagram was determined when the polymer-poor phase first occurred in a series of samples with increasing DMSO concentration.

2.3. Membrane preparation and characterization

Membranes were prepared using the direct immersion–precipitation method. An appropriate amount of EVAL was dissolved in DMSO to form a 20 wt% homogeneous solution. This solution was dispersed uniformly on a glass plate (ca. 100 μm), and then immersed into the nonsolvent bath to form membranes. Freeze-dried samples of the membranes were examined using a scanning electron microscope (SEM) to obtain the membrane structures.

2.4. Measurement of precipitation time

Light transmission experiments were performed to measure the time of the onset of precipitation due to phase separation in the membrane solution. A collimated light beam was directed to the membrane solution immersed in a nonsolvent bath. The light transmittance is recorded with a data acquisition system. The light intensity profiles are plotted as a function of time. The initial precipitation time is identified as the time at which transmission intensity starts to decrease. For detailed experimental setup and procedures, one can refer to the work of Reuvers et al. [5].

3. Results

3.1. Phase diagrams of water–DMSO–EVAL and 2-propanol–DMSO–EVAL

Phase diagrams of water–DMSO–EVAL and 2-propanol–DMSO–EVAL at 25°C are shown in Figs. 1 and 2, respectively. The data points, denoted by filled triangles and circles, represent the composition at which gelation (\blacktriangle) and two equilibrium liquid phases (\bullet) first occur in a

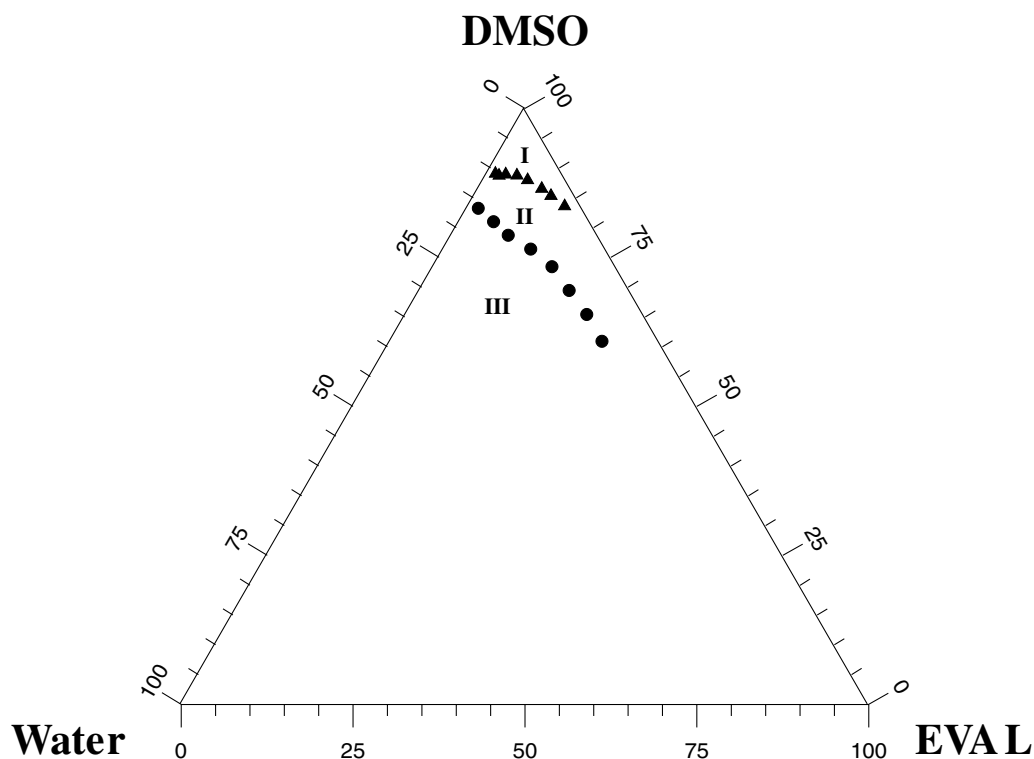


Fig. 1. Phase diagrams of water–DMSO–EVAL at 25°C [9]. Filled triangles (▲) represent the composition at which gelation occurs and filled circles (●) represent the compositions at which two liquid phases form.

series of samples with increasing nonsolvent concentration, respectively. Both phase diagrams show the gelation and binodal boundaries divide the phase diagram into three parts. Any solution in the region I, defined above the gelation boundary, is single-phase and homogeneous, i.e. EVAL is dissolved in such a mixture at higher solvent compositions. The region II, defined between the gelation and the binodal boundaries, is metastable with respect to pure EVAL. Any composition in this region will undergo solid–liquid demixing to form a gel that is crystalline EVAL dispersing uniformly in the liquid [9]. The region III, below the binodal boundary, is metastable with respect to both liquid–liquid demixing and crystallization. Actually, such a phase diagram represents two phase diagrams in the one figure; one approximates true equilibrium between EVAL solution and EVAL crystals and the other represents liquid–liquid demixing of the supersaturated liquid [11]. Hence, the phase diagrams that are drawn together in Figs. 1 and 2 for simplicity cannot really exist together. In general, initiation of liquid–liquid demixing is more rapid than nucleation of polymer crystallization that requires a rearrangement of polymer [15], so liquid–liquid demixing is kinetically favored to separate the supersaturated solution into two clear liquid phases. Subsequently, the polymer-rich phase will be always extremely supersaturated with respect to crystallization, thus, EVAL polymer eventually crystallize to form a white gel solid to coexist with a clear liquid phase. Conversely, if the crystallization is supposed to be a

faster process than liquid–liquid demixing at a high degree of supersaturation, then this solution could not undergo a further phase separation after crystallization. Consequently, no liquid–liquid demixing could be obtained experimentally at higher polymer concentration. This suggests that the liquid–liquid demixing data points only occur at lower polymer composition in the phase diagram, as indicated in Fig. 2.

3.2. Morphologies of membranes prepared from water–DMSO–EVAL and 2-propanol–DMSO–EVAL

The EVAL membrane, prepared by using water as the nonsolvent, shows an asymmetric structure consisting of a dense skin, and finger-like macrovoids and cellular morphologies between macrovoids in the sublayer, as indicated in Fig. 3. Typical morphology of polymer crystallization (i.e. particulate) as discussed in previous reports [11–14] is not evident in this membrane. Therefore, the phase separation process responsible for the observed membrane structure is liquid–liquid demixing. From the phase diagram shown in Fig. 1, however, it can be found that mass exchange of solvent and nonsolvent brings the membrane solution into a metastable state initially with respect to solid–liquid demixing, and then with respect to liquid–liquid demixing. In other words, it is expected that the membrane should exhibit a crystallization-controlled morphology. Hence, the membrane structure is contrary to

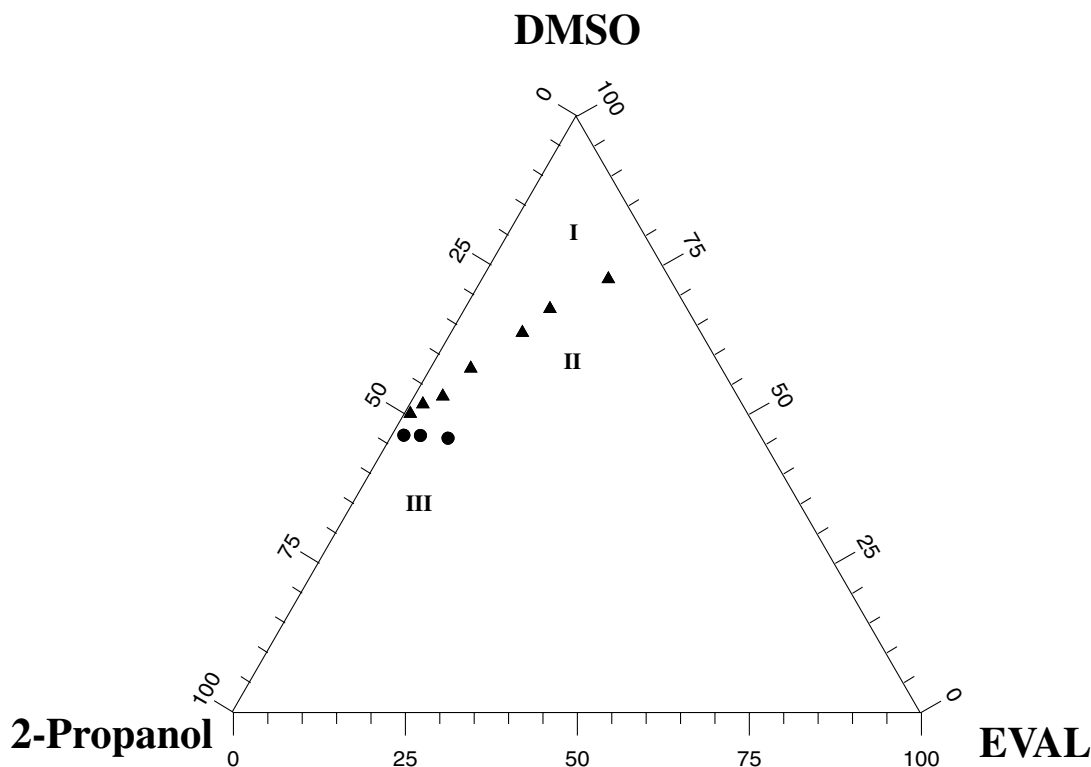


Fig. 2. Phase diagrams of 2-propanol–DMSO–EVAL at 25°C. Filled triangles (▲) represent the composition at which gelation occurs and filled circles (●) represent the compositions at which two liquid phases form.

the prediction on basis of the thermodynamic point of view. This suggests that liquid–liquid demixing can precede solid–liquid demixing even if solid–liquid demixing is favored thermodynamically.

The membrane, prepared by using 2-propanol as the nonsolvent, shows that the morphology is composed of particles with a diameter of approximately submicron order, as indicated in Fig. 4. The particle structure is representative of crystallization from a homogeneous mixture [11–14]. Qualitative comparisons of Fig. 4 with Fig. 3 indicate that the membrane precipitated in water has an asymmetric structure, while the connectedness of the membranes precipitated in 2-propanol arises from surface contact between particles. Figs. 1 and 2 indicate, however, the membrane solution is first metastable with respect to solid–liquid demixing, irrespective of immersing EVAL solution into water or 2-propanol. It is possible that if the diffusion is sufficiently fast to avoid crystallization in region II, then the binodal boundary of region III is crossed and the membrane structure is dramatically different. On the other hand, if the time is long enough to proceed solid–liquid demixing in region II, solid–liquid demixing takes place prior to liquid–liquid demixing during membrane formation. In the following paragraph, this difference in membrane structure prepared by using water and 2-propanol as the nonsolvent is discussed by taking into account the effect of the diffusion kinetics on the resulting membrane structure.

3.3. Precipitation time of membranes prepared from water–DMSO–EVAL and 2-propanol–DMSO–EVAL

Light transmission experiments were performed to measure the time of the onset of precipitation of the membrane solution in the nonsolvent bath. The principle of light transmission experiments is that the light transmittance of the membrane solution would decrease with the appearance of optical inhomogeneities, which can be induced by liquid–liquid demixing or solid–liquid demixing. The results of light transmission experiments for water and 2-propanol as the nonsolvents are shown in Fig. 5. Clearly, the instantaneous demixing via rapid exchange of nonsolvent and solvent takes place for water as the nonsolvent. Therefore, the obtained membrane structure using water as the nonsolvent was actually produced by liquid–liquid demixing. Conversely, it indicates a measured precipitation time of 13 s for 2-propanol as the nonsolvent, significantly longer than the instantaneous demixing case. Because of such postponement for the membrane formation process, nucleation of crystallites within the membrane solution may be feasible. As discussed below, the mechanism of phase separation significantly alters the resulting membrane structure.

4. Discussion

Since membrane preparation is a non-equilibrium

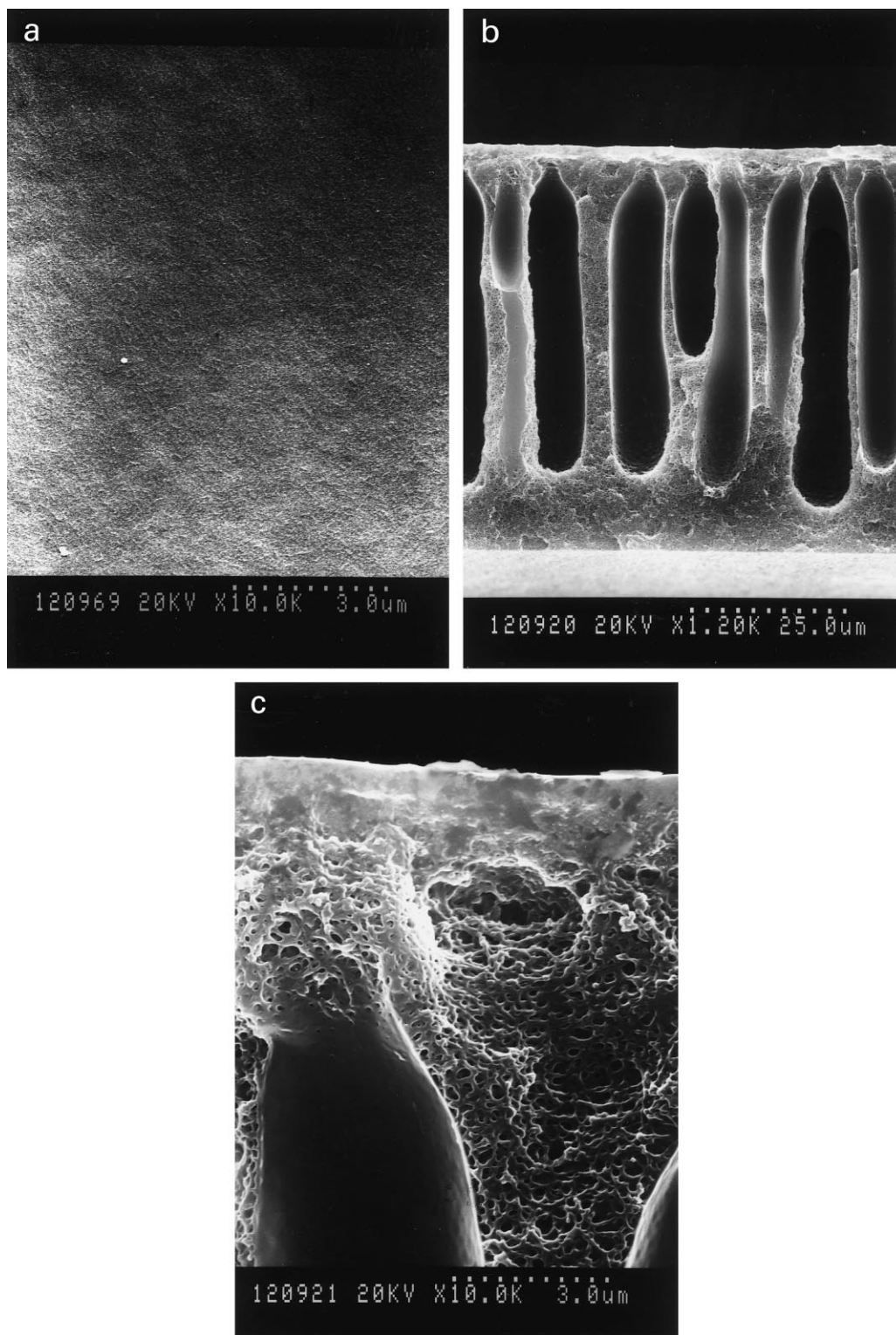


Fig. 3. SEM photograph of the EVAL membrane immersed in a water bath. (a) Top surface (original magnification $10,000\times$). (b) Cross-section (original magnification $1,200\times$). (c) The magnified photograph of (b) near the top layer (original magnification $10,000\times$).

process, it cannot be concluded that which one is favorable to proceed crystallization before liquid–liquid demixing occurs from the phase diagrams obtained by the two membrane formation systems in this work. In general, the

kinetic factor has a relatively minor effect on the liquid–liquid demixing. In contrast, the kinetic factor has a significant effect on the solid–liquid demixing. The reason for this consequence is that the actual rate at which polymer

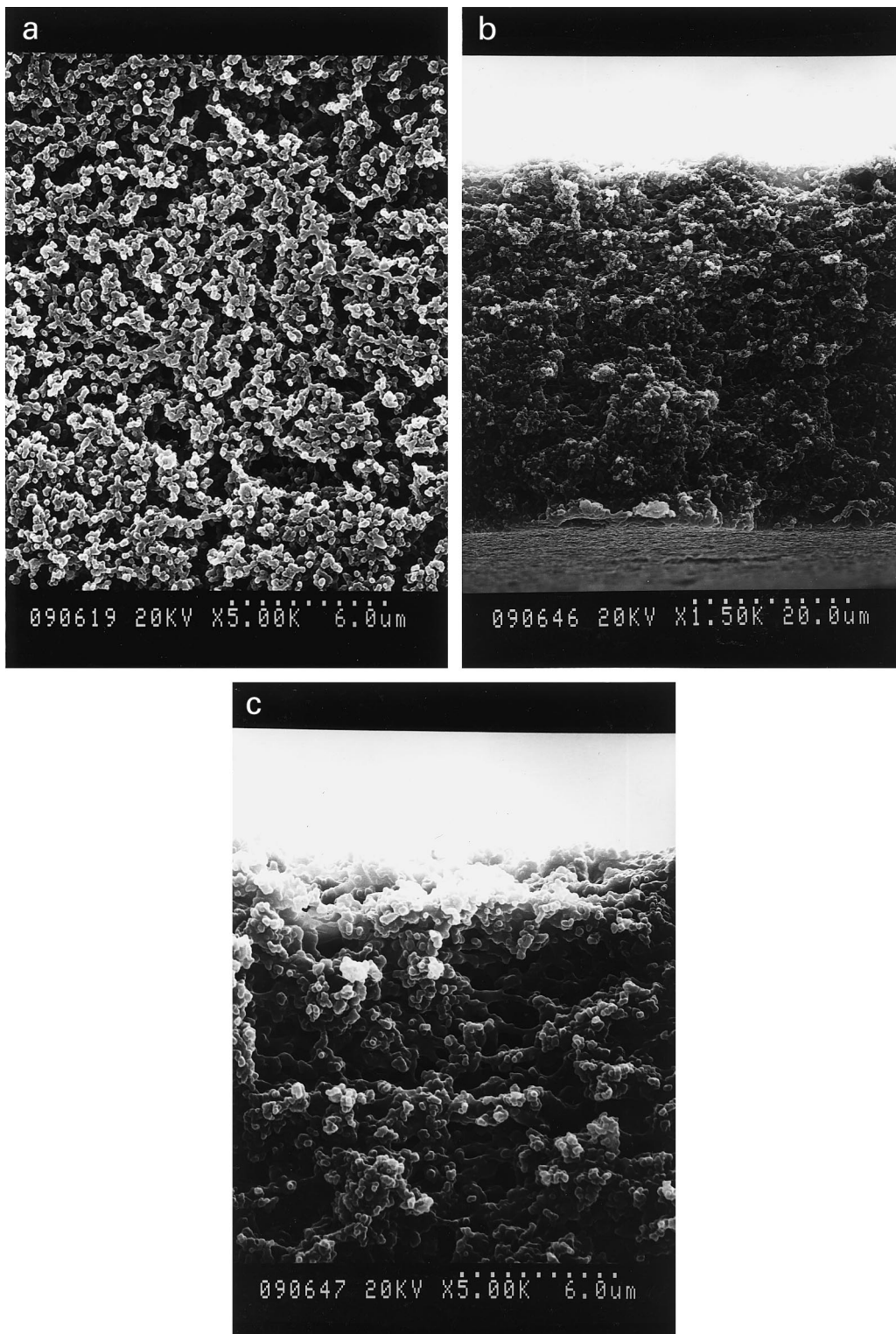


Fig. 4. SEM photograph of the EVAL membrane immersed in a 2-propanol bath. (a) Top surface (original magnification 5,000 \times). (b) Cross-section (original magnification 1,500 \times). (c) The magnified photograph of (b) near the top layer (original magnification 5,000 \times).

crystallizes depends on kinetic factors affecting the ability of successive atoms in the polymer molecule to move into successive positions in the crystal lattice. Therefore, increasing the diffusion rate of solvent and nonsolvent

permits supersaturation; that is, the membrane solution does not undergo the solid–liquid demixing below its corresponding equilibrium crystallization line in the phase diagram.

The kinetics of a ternary system can be examined by a simple light transmission technique as described above. According to work by Reuvers et al. [5], the membrane formation process may proceed in two different ways, that is delayed demixing and instantaneous demixing. In case of delayed demixing, there is a certain time interval between the moment of immersion of polymer solution in the nonsolvent bath and the onset of liquid–liquid demixing. Under these conditions a dense top layer and isolated pores in the sublayer are formed in the final membranes. In case of instantaneous demixing, liquid–liquid demixing occurs in the interfacial region when the polymer solution is contacted with the nonsolvent bath. Only a very thin and dense toplayer is formed, as compared to delayed demixing. Delayed demixing occurs when the interaction between solvent and nonsolvent is poor. On the contrary, instantaneous demixing occurs when the interaction between solvent and nonsolvent is strong. In our opinion, the model for two different types of demixing by Reuvers is based on a system of “amorphous” polymer. It cannot be reasoned that polymer has the crystallization capability during the membrane formation. In case of crystalline polymer, when the transmittance decreases as soon as the film is immersed in the nonsolvent bath, the type of demixing should be liquid–liquid demixing. When a delay time between immersion and decrease of transmittance is observed, the demixing process may be solid–liquid demixing since the crystallization needs a longer induction time. This means that rather low diffusion rates of solvent and nonsolvent are necessary to undergo solid–liquid demixing during crystalline membrane formation.

In Fig. 6, diffusion trajectories at different times are given for 20 wt% EVAL solution immersed in a 2-propanol bath. The calculated composition profiles were analyzed by using a ternary mass transfer model developed in our previous report [23]. (The case for 20 wt% EVAL solution immersed in water has been published in this reference.) A trajectory is the set of composition defined for the 32 layers of membrane solution at a specific time. The local composition in any layer of the membrane solution was assumed to be represented by a single average value. The interfacial composition of the membrane solution is located on the binodal, in accordance with the assumed equilibrium boundary condition. The input parameters for model computation can be found in Table 1. In addition, the calculated binodal and tie lines are shown in this figure together with the experimental data points. The interaction parameters employed in the binodal computation are given in Table 2, which was measured by following Young et al. [9].

Simulation was carried out on the evolution of the local concentration within the membrane solution assuming that precipitation did not occur and a single phase condition always prevailed. The trajectory X shown in Fig. 6 represents the local compositions within the membrane solution 13 s after immersion. The composition profile is located completely outside the liquid–liquid demixing region.

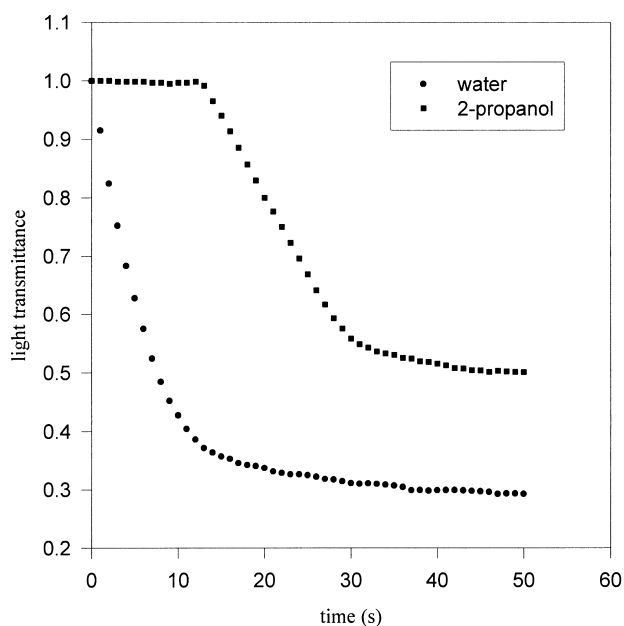


Fig. 5. Light transmission during immersion of EVAL solutions into water and 2-propanol baths.

Such a composition profile characterizes delayed liquid–liquid demixing. Comparing with the 13 s time measured from light transmission, it suggests that the observed precipitation was not a result of the liquid–liquid demixing process. By contrast, it can be seen the binodal was crossed right after immersion for 20 wt% EVAL solution immersed in a water bath (Fig. 3 in Ref. [23]). Such is a case termed “instantaneous demixing”.

Furthermore, the trajectory Y shown in Fig. 6 represents the local compositions within the membrane solution when the top interface just entered the binodal miscibility envelop at 72 s after immersion, significantly longer than the instantaneous demixing cases. Since liquid–liquid demixing process was sufficiently suppressed and the whole membrane solution was notably supersaturated with respect to crystallization, solid–liquid demixing process had the possibility to be responsible for the observed turbidity in the light transmittance measurement. Actually, our previous publication has confirmed that about 10–20 s are long enough for EVAL crystallization to occur in a water precipitation bath containing a substantial amount of DMSO [23]. Therefore, the time available for the membrane solution within the solid–liquid demixing region is large enough to initiate the solid–liquid demixing process. Because crystallization initiates the precipitation process, it dominated the precipitation process. Consequently, the formed membrane exhibits a typical particulate morphology characteristic of EVAL crystallization as shown in the membrane top and cross-sectional regions.

Finally, the cloud-point due to liquid–liquid demixing can be obtained up to 30% of EVAL for the system with water (Fig. 1) but only up to 10% for the system with 2-propanol (Fig. 2). The disappearance of liquid–liquid

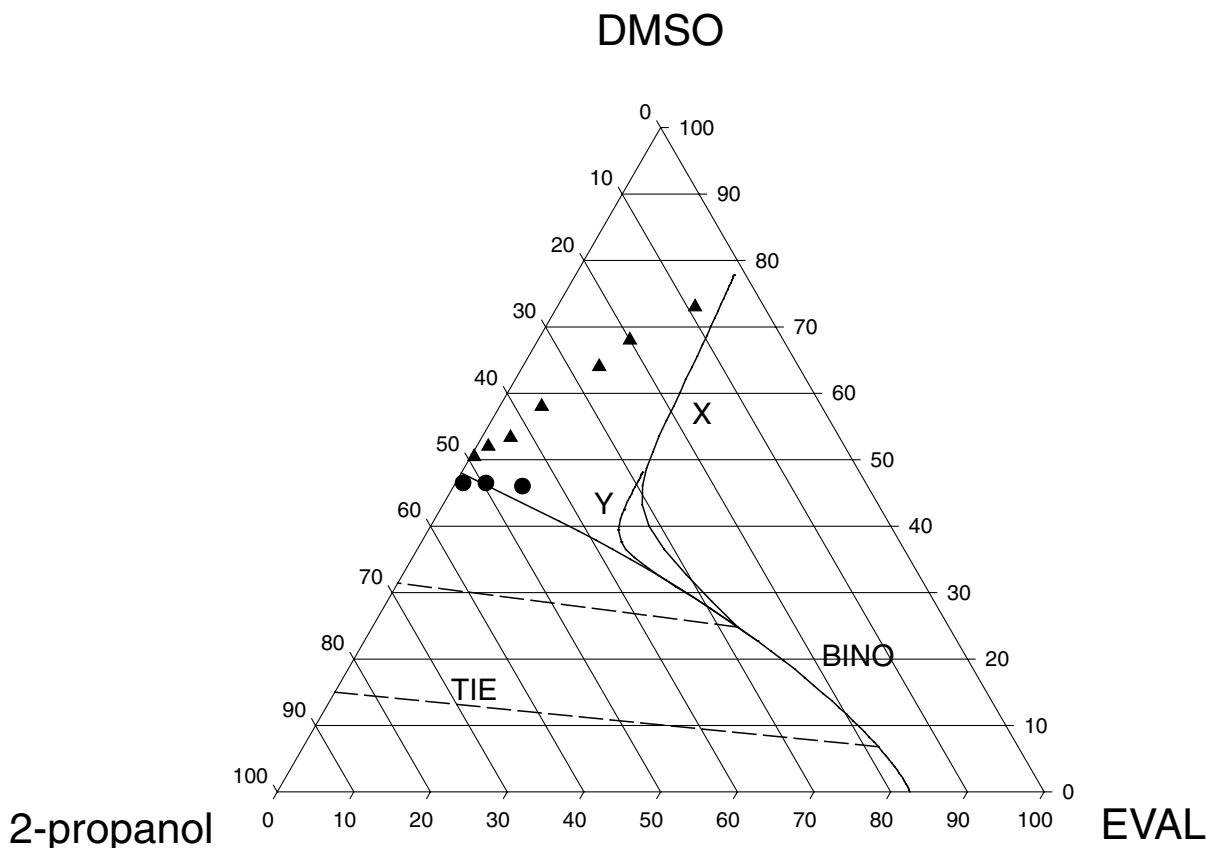


Fig. 6. Calculated diffusion trajectories for 20 wt% EVAL solution immersed in a 2-propanol bath. Filled triangles (▲) represent the composition at which gelation occurs and filled circles (●) represent the compositions at which two liquid phases form. BINO and TIE are binodal and tie lines calculated from experimental data by using the method developed in our previous report [9]. Trajectories: X at 13 s; Y at 72 s.

demixing with increasing polymer concentrations is a commonly observed phenomenon and can be attributed to the fact that the crystallization rate increases at increasing polymer concentration. This indicates, without consideration of diffusion kinetics, the system with 2-propanol is easier for EVAL to crystallize than the system with water. Overall, the system with 2-propanol has a longer delay time and a better crystallization capability than with water to

undergo the favorable phase separation (solid–liquid demixing) before enough solvent is depleted from or enough nonsolvent enters into the polymer solution to give liquid–liquid demixing.

5. Conclusions

In this paper we measured the phase diagrams of the ternary system water–DMSO–EVAL and 2-propanol–DMSO–EVAL, which were discussed in relation to the formation and morphologies of EVAL membranes. However, only equilibrium thermodynamic considerations are not enough to facilitate the explanation of the difference of the dynamic membrane formation process since the equilibrium crystallization lines are always located at higher

Table 1

Physical parameters for diffusion trajectory calculation of 20 wt% EVAL solution immersed in a 2-propanol bath at 25°C ($i = 1$, 2-propanol; $i = 2$, DMSO; $i = 3$, EVAL; ν , kinematic viscosity of 2-propanol and DMSO solution; V_i , molar volume of component i ; ϕ_i , volume fraction of component i ; mutual diffusivity of 2-propanol and DMSO (D_{12}) was obtained by linear regression from their diffusion coefficients at infinite dilution. Other parameters were obtained from Ref. [23])

Parameter	2-Propanol–DMSO–EVAL system
Initial thickness (μm)	100
ν (cm^2/s)	0.023
V_1 (cm^3/mol)	76.56
V_2 (cm^3/mol)	70.96
V_3 (cm^3/mol)	47.836
D_{12} (cm^2/s)	$1.8 \times 10^{-5} - 1.169 \times 10^{-5} \phi_1$

Table 2

Summary of interaction parameters for 2-propanol–DMSO–EVAL at 25°C ($i = 1$, 2-propanol; $i = 2$, DMSO; $i = 3$, EVAL; ϕ_i , volume fraction of component i ; $h_2 = \phi_2/(1 - \phi_3)$)

Binary system	Interaction parameter
2-Propanol–DMSO	$0.11 - 1.376/(1.0 + 0.702h_2)$
2-Propanol–EVAL	1.35
DMSO–EVAL	$-1.0 + 0.9\phi_3$

solvent concentrations than the binodal boundaries in these two phase diagrams. Equilibrium crystallization line in a ternary phase diagram represents a polymer can crystallize in such an environment, but it cannot predict its rate. When the membrane solution transverses the equilibrium crystallization line, crystallization probably will not occur. The solution remains homogeneous until the liquid–liquid binodal is crossed. From the kinetic point of view, the degree of supersaturation, necessary to form crystal nuclei, increases with increasing polymer concentration. Therefore, the role of solid–liquid demixing processes for a membrane formation system can be related to the rate of solvent/nonsolvent exchange. When water was used as a nonsolvent, the membrane solution transverse the crystallization line without crystallization due to fast diffusion. This results in a traditional asymmetric membrane. On the other hand, when 2-propanol was used as a nonsolvent, EVAL has enough time to proceed solid–liquid demixing due to slow diffusion, which was in reasonable agreement with the observed membrane structure with crystallization-controlled morphologies. Therefore, an important factor determining whether solid–liquid or liquid–liquid demixing occurs for a system involving a semicrystalline polymer is the diffusion kinetics of the system.

Acknowledgements

The authors thank the National Science Council of the Republic of China for their financial support of project NSC 89-2216-E-002-006.

References

- [1] Altena FW, Smolders CA. *Macromolecules* 1982;15:1491.
- [2] Yilmaz L, McHugh AJ. *J Appl Polym Sci* 1986;31:997.
- [3] Cohen C, Tanny GB, Prager SJ. *J Polym Sci A-2* 1979;17:477.
- [4] Yilmaz L, McHugh AJ. *J Membr Sci* 1986;28:287.
- [5] Reuvers AJ, van der Berg JWA, Smolders CA. *J Membr Sci* 1987;34:45.
- [6] Radov P, Thiel SW, Hwang ST. *J Membr Sci* 1992;65:213.
- [7] Cheng LP, Dwan AW, Gryte CC. *J Polym Sci: Polym Phys* 1995;33:211.
- [8] Cheng LP, Dwan AW, Gryte CC. *J Polym Sci: Polym Phys* 1995;33:223.
- [9] Young TH, Lai JY, Yu WM, Cheng LP. *J Membr Sci* 1997;128:55.
- [10] Young TH, Cheng LP, Hsieh CC, Chen LW. *Macromolecules* 1998;31:1229.
- [11] Aubert JH. *Macromolecules* 1988;21:3468.
- [12] Lloyd DR, Kinzer KE, Tseng HS. *J Membr Sci* 1990;52:239.
- [13] Bulte AMW, Folkers B, Mulder MHV, Smolders CA. *J Appl Polym Sci* 1993;50:13.
- [14] van de Witte P, Esselbrugge H, Dijkstra PJ, van de Berg JWA, Feijen J. *J Polym Sci: Polym Phys* 1996;34:2569.
- [15] Reuvers AJ, Altena FW, Smolders CA. *J Polym Sci: Polym Phys* 1986;24:793.
- [16] Bulte AMW, Mulder MHV, Smolders CA, Strathmann H. *J Membr Sci* 1996;121:37.
- [17] Yamashita S, Nagata S, Takakura K. US Patent, 4,134,837, 1979.
- [18] Sakurada Y, Sueoka A, Kawahashi M. *Polym J* 1987;19:501.
- [19] Cheng LP, Lin HI, Chen LW, Young TH. *Polymer* 1998;39:2135.
- [20] Lin DT, Cheng LP, Kang YJ, Chen LW, Young TH. *J Membr Sci* 1998;140:185.
- [21] Nakamae K, Kameyama M, Matsumoto T. *Polym Engng Sci* 1979;19:572.
- [22] Apicella A, Hopfenberg HB, Piccarolo S. *Polym Engng Sci* 1982;22:382.
- [23] Cheng LP, Young TH, You WM. *J Membr Sci* 1998;145:77.